Bond of FRP Strengthening Systems for Concrete Structures: A Round Robin Test

M. Guadagnini & A. Serbescu
The University of Sheffield, Sheffield, UK

A. Palmieri & S. Matthys
Ghent University, Ghent, Belgium

A. Bilotta & E. Nigro
University of Naples, Naples, Italy

C. Mazzotti
University of Bologna, Bologna, Italy

G. Sas, B. Taljsten
University of Lulea, Lulea, Sweden

F. Ceroni
University of Sannio, Sannio, Italy

C. Czaderski & S. Olia
Laboratory EMPA, Dübendorf, Switzerland

Z. Szabo & G. Balazs
University of Budapest, Budapest, Hungary

J. Barros & I. Costa
University of Minho, Guimarães, Portugal

V. Tamuzs
University of Latvia, Riga, Latvia

ABSTRACT: Although various test methods to examine the local bond behaviour of FRP strengthening systems to concrete have been proposed thus far, their implementation can lead to a wide range of results and a standard methodology has yet to be generally accepted. With these issues in mind, a Round Robin Testing (RRT) programme was carried out to assess the performance and reliability of small scale testing on various FRP strengthening systems, including both externally bonded laminates and near surface mounted reinforcement. Ten laboratories and eight manufacturers and suppliers participated in this extensive international exercise, which was initiated within the framework of the European funded Marie Curie Research Training Network, EN-CORE, with the support of Task Group 9.3 of the International Federation for Structural Concrete (fib). This paper describes the proposed testing programme and summarized some of the results obtained by the participating laboratories.

1 INTRODUCTION

Since their first application in civil engineering projects, FRP materials have been successfully used to develop innovative strengthening solutions and, over the last decade, the interest in using these advanced materials for the rehabilitation of structurally deficient concrete bridges has increased dramatically. FRPs can be used to increase the flexural, shear and torsional capacity of RC elements (e.g. concrete box girders) and a variety of systems are commercially available, including externally bonded and near surface mounted solutions.

Unless specific anchorage systems are used (e.g. Williams et al. 2010), the bond of the FRP system to the concrete substrate can limit the effectiveness of the adopted strengthening solution and lead to poor material utilization.

Bond behavior of FRP to concrete is still not well understood and, although several design models have been developed to predict the load causing debonding of FRP strengthening systems, particularly externally bonded, these are based on purely empirical approaches (e.g. Chen & Teng 2001) or rely on observations and results obtained from small scale testing (e.g. Dai et al. 2005).

Various test methods have been proposed to date to examine the local bond behaviour of FRP systems bonded to concrete (e.g. Yao et al. 2005), but their implementation can lead to a wide range of results and a standard methodology has yet to be generally accepted. A reliable determination of the bond behaviour between an FRP system and concrete is therefore critical for the optimal design and detailing of a strengthening solution. With these issues in mind, a Round Robin Testing (RRT) programme was conducted to assess the performance and reliability of small scale testing on externally bonded and near surface mounted FRP strengthening systems. This extensive international exercise was initiated within the framework of the European funded Marie Curie Research Training Network, EN-CORE, and completed with the support of Task Group 9.3 of the International Federation for Structural Concrete (*fib*).

Ten laboratories and eight manufacturers and suppliers participated in this extensive international exercise aimed at examining the reliability of the test methods that are most commonly used for the characterization of FRP strengthening systems. The overall test programme comprised four test series: 1) tensile tests on FRP bars and strips; 2) tensile tests on FRP laminates; 3) bond tests on externally bonded (EBR) laminates; and 4) bond tests on near surface mounted (NSM) bars and strips. Only test series 3 and 4, however, which were carried out at eight of the participating laboratories, is presented herein.

The test methodology that was implemented to conduct the required bond tests is described below and the results are summarized and briefly discussed. The influence of various parameters, including the effect of different test setups, is commented upon.

2 EXPERIMENTAL PROGRAMME

Six different CFRP externally bonded strengthening systems (see Table 1) and eight NSM bars/strips (see Table 2) were tested. A minimum of 2 tests per strengthening system were carried out at each laboratory for a total of 180 tests (89 on EBR and 91 on NSM reinforcement – see Table 4).

2.1 *Material properties and specimen preparation*

The geometrical and mechanical properties of the tested FRP laminates, bars and strips are presented in Tables 1 and 2 in terms of average width, w_f; thickness, t_f; area, A_f; bar diameter or strip cross section, d_f; ultimate strength, f_f; Young's modulus, E_f; and ultimate strain, ε_f. Details on the surface finish of the bars/strips used as NSM systems are also reported along with the dimensions of the grooves provided to mount the FRP reinforcement. The first letter of the specimen ID indicates the type of FRP material (B = basalt; C = carbon; G = glass). The average cube strength of the concrete used to manufacture the specimens, f_{cu}, varied from 23MPa to a maximum of 42MPa (see Table 3).

Table 1. Mechanical and physical properties of FRP laminates.

ID	w_f [mm]	t_f [mm]	A_f [mm^2]	f_f [MPa]	E_f [GPa]	ε_f [%]
C1A	100	1.2	120	3100	165	1.7
C1B	100	1.4	140	3100	210	1.35
C1C	60	1.3	78	3100	165	1.7
C2	100	1.0	100	2850	175	-
C3	100	1.2	120	2900	165	-
C4	100	1.4	140	3100	170	1.6

Table 2. Mechanical and physical properties of FRP bars/strips.

ID	Surface Finish*	d_f [mm]	Groove [mm]	f_f [MPa]	E_f [GPa]
C-6-SC	SC	6.0	12x12	2068	124
B-6-SC	SC	6.0	12x12	1413	50
B-8-SC	SC	8.0	14x14	1208	50
C-1.4x10-S	S	1.4x10	5x15	1850	50
G-8-RB	RB	8.0	14x14	1500	60
C-2.5x15-S	S	2.5x15	8x25	3100	165
C-8-S	S	8.0	14x14	2800	155
C-10x10-S	S	10x10	15x15	2000	155
G-8-SW	SW	8.0	12x12	1333	52

* SC = Sand coated; RB = ribbed; S = smooth; SW = spiral wound

A double shear test (DS) or a single shear test (SS) setup was adopted according to the specifications summarized in Figures 1-4. The specimens used for DS tests comprised two concrete prisms (400x150x150mm), whilst one concrete prism (400x200x160mm) was used for SS tests. One or two steel bars were embedded in the concrete prisms to allow anchorage or application of load. Special care was taken when preparing the specimens for DS tests to guarantee the alignment of the embedded bars so as to minimize any possible problem due to load eccentricity during testing.

A bonded length of 300mm was chosen to ensure the development of the maximum anchorable force for each of the tested systems according to fracture mechanics approaches (fib 2001). A 50mm long region was left unbonded at the loaded end of both EBR and NSM systems to prevent the development of high shear stresses in this region and avoid premature local damage of the concrete.

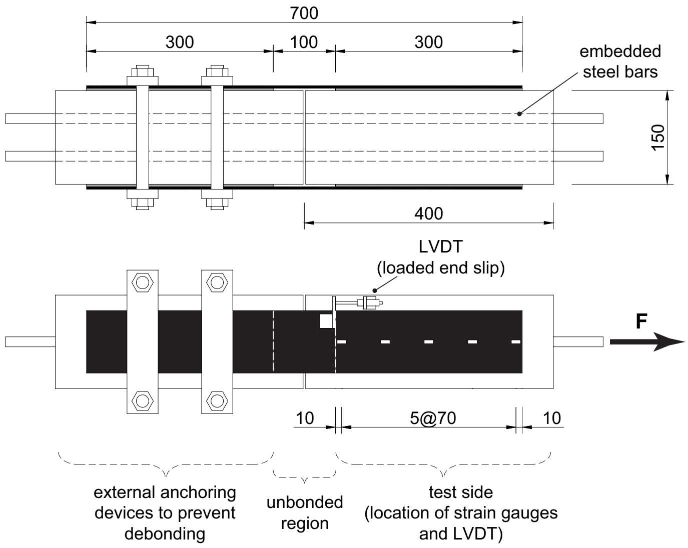

Figure 1. Typical test setup for double shear tests (DS) on EBR.

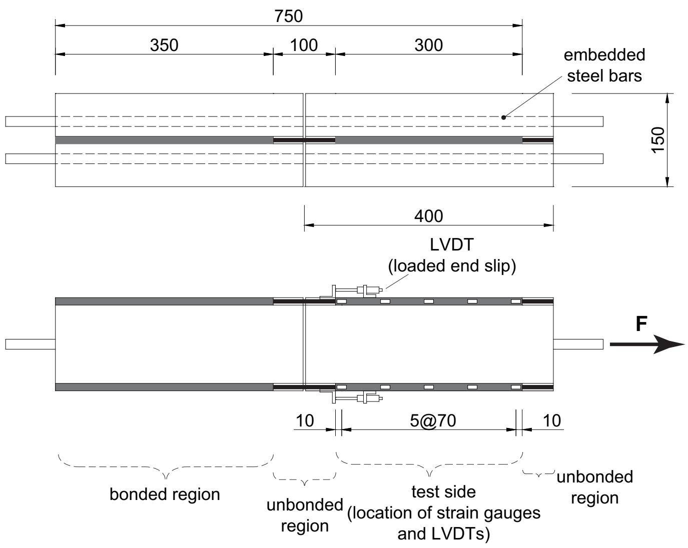

Figure 2. Typical test setup for double shear tests (DS) on NSM.

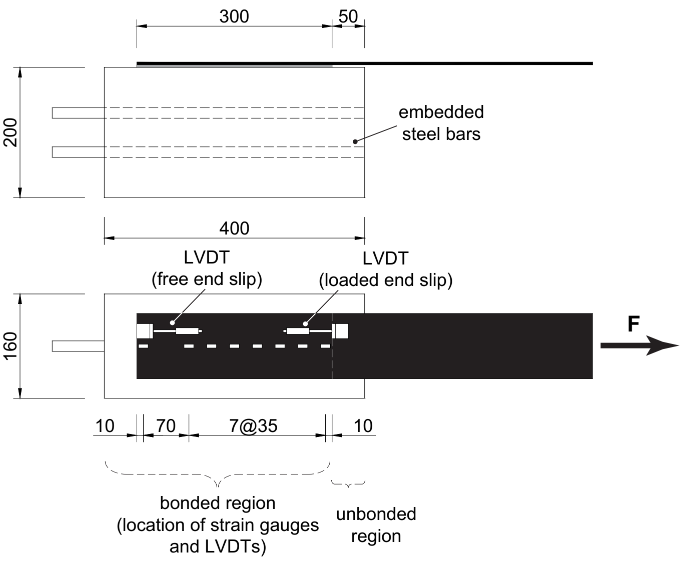

Figure 3. Typical test setup for single shear tests (SS) on EBR.

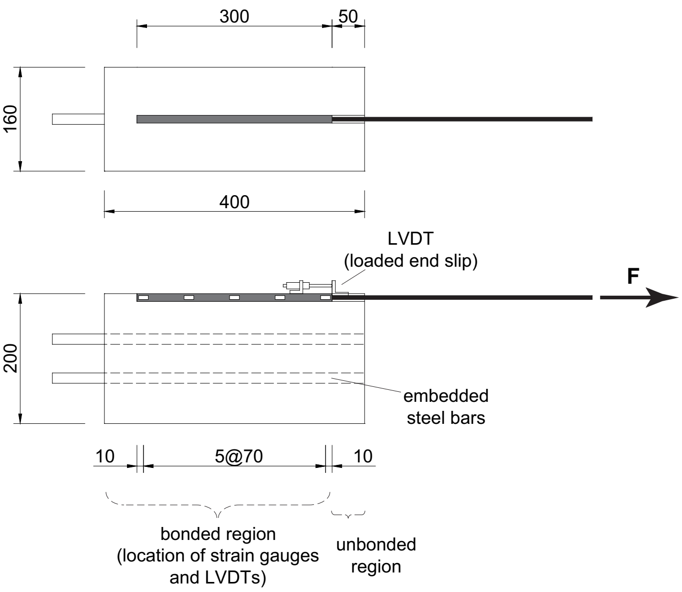

Figure 4. Typical test setup for single shear tests (SS) on NSM.

Pryor to the application of the adhesive layer, the concrete substrate of the specimens to be used for EBR systems was prepared as specified in Table 3. A diamond blade saw was used to cut the grooves in the concrete prisms to be used for the NSM systems and compressed air or water was used to remove dust particles. No additional surface treatment was applied to these specimens.

When a DS configuration was employed, external anchoring devices (for EBR systems) or longer bonded lengths of 350mm (for NSM systems) were used to provide additional bond capacity to one half of the specimen and promote failure on the opposite, instrumented side.

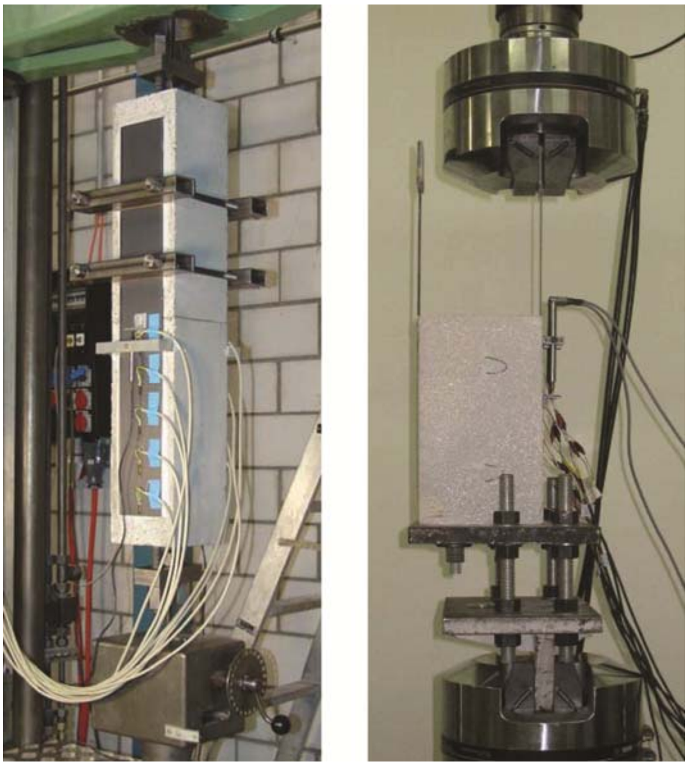

Figure 5. Example of setups used for DS (left) and SS (right) tests on EBR systems.

Figure 6. Example of setups used for DS (left) and SS (right) tests on NSM systems.

2.2 *Test setup and instrumentation*

Although some minor adjustments were implemented at the various laboratories (e.g. number and location of strain gauges and LVDTs), the tests were designed to subject the concrete prisms to a tension-tension state of stress (i.e. pull-pull shear tests).

Table 3. Summary of main procedural differences between testing laboratories.

Testing Laboratory	Type of Test*	Loading Rate [mm/min]	f_{cu}** [MPa]	Embedded Steel Bars n°/diam (mm)	Concrete Surface Preparation***
Sheffield	DS	0.05	27	2/16	Wire brushing
Ghent	DS	0.1	32	2/16	Grinding
Naples/Sannio	SS	0.18	23	2/20	Bush hammering
Empa	DS	0.5	41	2/16	Abrading
Budapest	DS	2	42	1/18	No treatment
Bologna	SS	1.2	23	2/20	Bush hammering
Minho	DS	1.0	35	2/16	-

* DS = Double Shear Test; SS = Single Shear Test - ** average values - *** for tests on EB systems only

Table 4. Number of tests carried out at participating laboratories on selected strengthening systems.

Testing Laboratory	Externally Bonded						Near Surface Mounted								
	C1A	C1B	C1C	C2	C3	C4	C-6 -SC	B-6 -SC	B-8 -SC	C-1.4 ×10-S	G-8-RB	C-2.5 ×15-S	C-8 -S	C-10 x10-S	G-8 -SW
Sheffield	3	3	3	-	3	3	-	-	-	-	-	-	-	-	-
Ghent	3	3	3	3	3	3	2	2	-	3	2	3	3	2	-
Naples/Sannio	3	3	3	3	3	3	3	3	3	3	3	3	3	3	-
Empa	2	-	-	2	2	2	-	-	-	-	-	-	-	-	-
Budapest	-	3	3	3	-	3	3	3	3	2	3	3	3	3	3
Bologna	3	3	3	3	3	3	-	-	-	-	-	-	-	-	-
Minho	-	-	-	-	-	-	-	3	3	3	3	3	3	3	3
Total	14	15	15	14	14	17	8	11	9	11	11	12	12	11	6

The steel bars embedded in the concrete prisms were used to fix the specimens in the grips of the testing machine and, in the case of DS tests, also to apply the external tensile load. When the SS setup was implemented, the load was applied to the FRP reinforcement via a pair of steel plates or tubes bonded to the FRP to avoid local crushing.

A minimum of 5 strain gauges and 1 LVDT were used to monitor the development of strains along the bonded portion of the FRP reinforcement, and the loaded end slip, respectively (see Figures 5 and 6 for more details). All of the tests were conducted in displacement control with loading rates varying from 0.05mm/min to 2mm/min (see Table 3).

3 SUMMARY OF RESULTS

Although the behaviour of the test specimens was monitored through the use of an extensive array of instrumentation, the discussion in the following section will be limited to the presentation of failure modes and overall performance in terms of average bond stress.

3.1 *Externally bonded strengthening systems*

3.1.1 *Failure modes*

The type of failure that was predominantly observed in this series of tests was characterized by debonding in the concrete adjacent to the adhesive-concrete interface (Figure 7). This was evidenced by a thin layer of concrete still bonded to the FRP laminate after failure. Splitting-related failures were observed in few of the specimens tested in either a DS or SS configuration (Figure 8). Some of the specimens tested in SS exhibited splitting and separation of a concrete wedge from the frontal, loaded region of the specimen.

3.1.2 *Bond behaviour*

The average bond strength, τ_m, developed by the tested strengthening systems is summarized in Table 5 and Figure 9. These average values have been determined as:

$$\tau_m = \frac{P_{\max}}{l_b \cdot b_f} \qquad (1)$$

where P_{max} = maximum load applied to one laminate; l_b = initial bonded length provided (i.e. 300mm); and b_f = width of the laminate. Table 5 also includes the coefficient of variation calculated for each set of specimens across the various laboratories, while the standard deviation observed at individual laboratories for each set of specimens is represented graphically through error bars in Figure 9. The data presented in Table 5 and Figure 9 show that the experimentally determined average bond strength values are affected by a considerably large scatter. The observed scatter reduces, however, when the results of tests carried out on specimens with minimal or no surface preparation are excluded.

Figure 10 compares the results obtained for specimens C4 in terms of average bond stress and loaded end slip. It can be seen that overall responses can vary significantly between laboratories, though maintaining a distinctive behaviour depending on surface preparation.

3.2 *Near surface mounted reinforcement*

3.2.1 *Failure modes*

The most observed type of failure was by debonding at the concrete-epoxy interface, with varying degrees of concrete damage (see for example Figure 11). Other types of failure, however, were also observed, including debonding at the FRP-epoxy interface, longitudinal splitting of the epoxy, splitting of the concrete specimens, bar/strip pullout (see for example Figure 12), as well as tensile failure of the FRP reinforcement. In addition, not all of the specimens tested in the DS configuration failed by debonding along the monitored side, with a relatively small percentage failing on the opposite side, where a longer embedded length was provided.

Figure 7. Typical failures due to debonding in the concrete adjacent to the adhesive-concrete interface.

Figure 8. Observed splitting-related failures in EBR specimens.

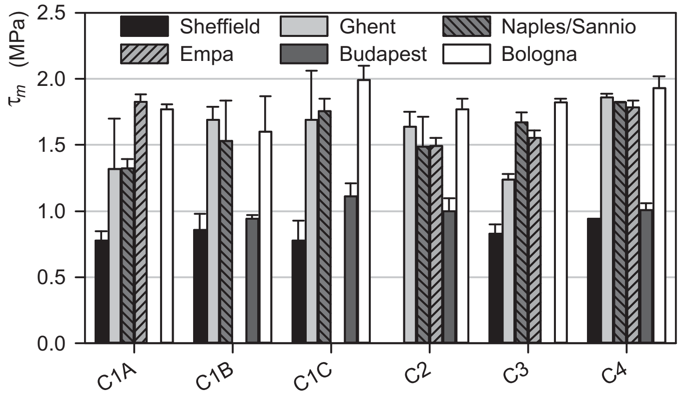

Figure 9. Average bond strength of the tested EBR systems (error bars represent one standard deviation).

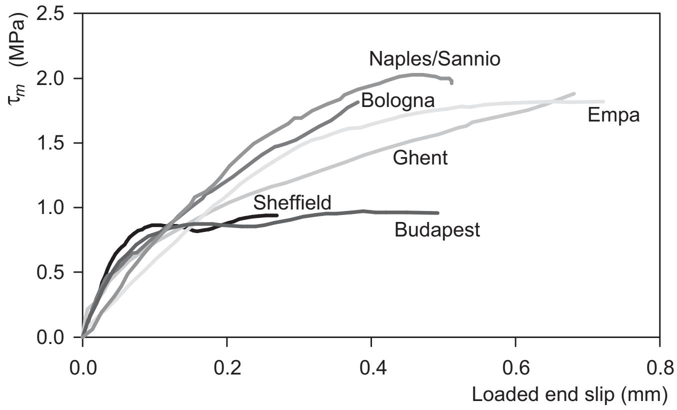

Figure 10. Bond slip behaviour of EBR specimens C4.

The variability in the mode of failure was observed not only across the various specimens tested at each of the participating laboratories, but also within the tests carried out on the same NSM system at the various laboratories. This has also contributed to affecting the reliability of the obtained results, showing a high scatter.

Table 5. Average bond strength of the EBR tested systems. All values in MPa unless otherwise indicated.

TESTING LABORATORY	C1A	C1B	C1C	C2	C3	C4
Sheffield	0.8	0.9	0.8	-	0.8	0.9
Ghent	1.3	1.7	1.7	1.6	1.2	1.9
Naples/Sannio	1.3	1.5	1.8	1.5	1.7	1.8
Empa	1.8	-	-	1.5	1.6	1.8
Budapest	-	0.9	1.1	1.0	-	1.0
Bologna	1.8	1.6	2.0	1.8	1.8	1.9
Average*	1.4 (1.6)	1.3 (1.6)	1.5 (1.8)	1.5 (1.6)	1.4 (1.6)	1. 6 (1.8)
COV* [%]	30.1 (17.7)	29.6 (4.9)	34.2 (8.7)	19.7 (8.4)	27.7 (15.7)	29.2 (3.4)

* figures in brackets do not include results for specimens with no/minimal surface preparation

Figure 11. Typical failures of NSM specimens with varying degrees of concrete damage.

3.2.2 *Bond behaviour*

The maximum average bond strength, τ_m, developed by the tested NSM systems is summarized in Table 6 and Figure 13. These average values have been determined according to Equations 2 or 3.

$$\tau_m = \frac{P_{\max}}{l_b \cdot p_b} \quad \text{if failure at FRP/epoxy interface} \tag{2}$$

$$\tau_m = \frac{P_{\max}}{l_b \cdot p_g} \quad \text{if failure at epoxy/concrete interface} \tag{3}$$

where P_{max} = maximum load applied to one bar/strip; l_b = initial bonded length provided (i.e. 300mm); p_b = perimeter of the bar/strip; and p_g = length of the groove in cross section.

As for the results on EBR systems, Table 6 includes the coefficient of variation calculated for each set of specimens across the various laboratories, while the standard deviation observed at individual laboratories for each set of specimens is represented graphically through error bars in Figure 13.

Figure 12. Splitting-related (top) and pullout (bottom) failures in NSM specimens.

Table 6. Average bond strength of the NSM tested reinforcements. All values in MPa unless otherwise indicated.

Testing Laboratory	C-6-SC	B-6-SC	B-8-SC	C-1.4×10-S	G-8-RB	C-2.5×15-S	C-8-S	C-10×10-S	G-8-SW
Budapest	6.0	4.1		3.7	6.0	3.9	5.5	2.0	
Ghent	3.1	5.0	5.3	3.6	6.9	5.7	7.5	4.7	5.8
Minho	6.5	4.7	4.4	5.7	5.4	4.6	6.3	4.9	
Naples/Sannio		3.7	2.5	3.1	3.8	3.0	3.9	3.7	4.3
Average	5.2	4.4	4.1	4.0	5.5	4.3	5.8	3.8	5.0
COV [%]	35.9	14.0	34.8	28.5	23.6	27.0	25.9	35.3	21.4

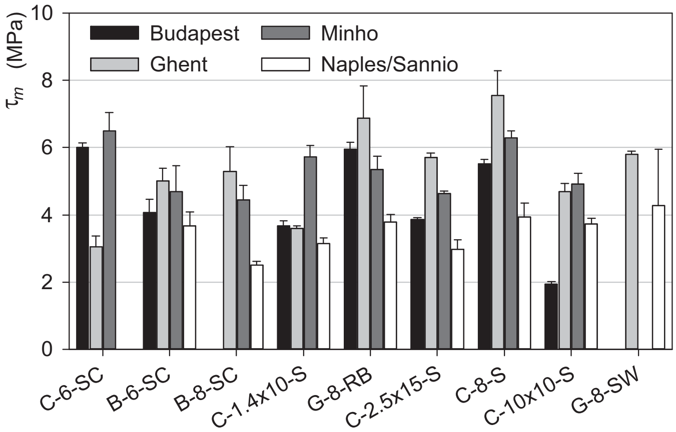

Figure 13. Average bond strength of the NSM tested reinforcements (error bars represent one standard deviation).

Figure 14 compares the results obtained for specimens G-8-RB in terms of applied load and loaded end slip, whilst the same information is relayed in terms of bond-slip behaviour in Figure 15. The type of failure reported by the testing laboratories is also indicated in Figure 14, where Cls/Epx = debonding at the concrete-epoxy interface; Epx.split = longitudinal splitting of the epoxy. As failure of these specimens was characterized by the development of different mechanisms, the overall responses varied accordingly. This particular example also illustrates how the observed failure mode can affect the determination of data that are calculated from experimental results, namely the average bond stress (see Eqs. 2 and 3 and compare Figures 14 and 15).

4 DISCUSSION

Although the COV of the results of tests on both EBR and NSM systems at an individual laboratory was typically around 10%, this could increase to more than 35% when all of the results across the participating laboratories are taken into account. This can be attributed to a series of factors, including variability of concrete, surface preparation, load misalignment. The preparation of specimens to be tested in a DS configuration has proven cumbersome, mainly in terms of ensuring the alignment of the two prisms and of the embedded steel reinforcement, as did the handling of the specimens. If similar conditions are provided, however, the use of a DS or an SS configuration does not seem to affect overall performance and behavior to a great extent. The number of specimens exhibiting concrete splitting related failures, however, was comparatively higher for SS tests than for DS tests. This could be attributed to the possible effects of load eccentricity, but also to the lower concrete strength used for the specimens tested in this configuration.

Owing to the development of relatively higher bond stresses along the NSM systems, and the interaction with the stresses developed along the embedded steel bars, the occurrence of splitting-related type of failures was comparatively higher in tests on NSM systems than on EBR systems.

The way in which slip is measured can affect considerably the results and their interpretation. As it is not easy to decouple the elastic deformation of the unbonded portion of the composite from the total, measured deformation, the use of strain gauges along the FRP reinforcement provides more reliable measurements that can be used to determine local slips, as well as the variation of local bond stresses.

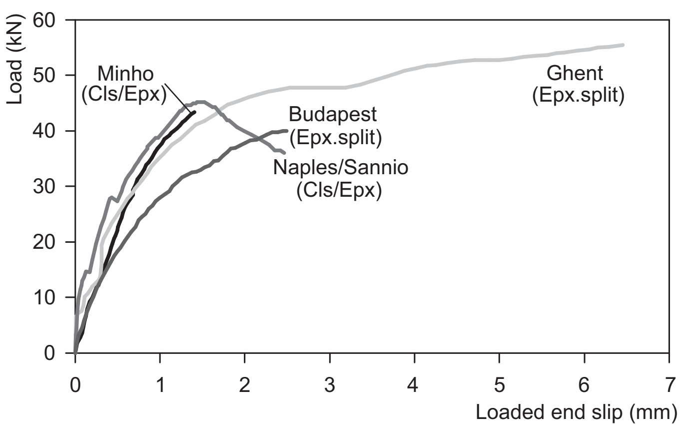

Figure 14. Load slip behaviour of specimens G-8-RB. Observed failure modes are indicated in brackets.

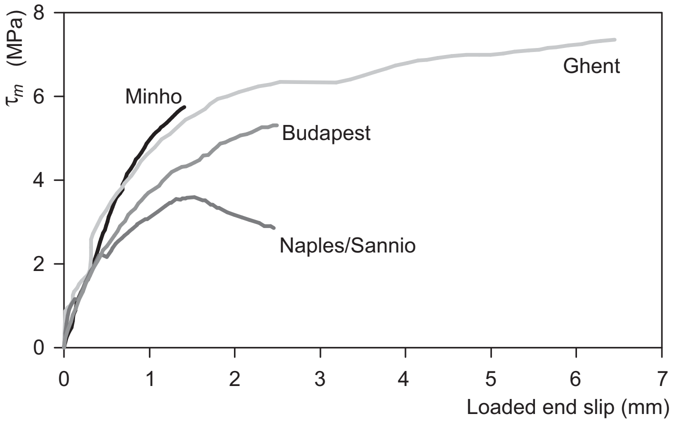

Figure 15. Bond slip behaviour of specimens G-8-RB

5 CONCLUDING REMARKS

Although this paper has only briefly discussed some of the results obtained from the extensive experimental programme discussed herein, the following considerations can be made.

The lack of a reliable standard methodology for the determination of the bond behaviour of FRP strengthening systems is hindering the development of more sophisticated models that can be used for analysis and design.

The quality of the concrete substrate, primarily in terms of surface finish, can affect bond behaviour of EBR systems to a large extent.

The preparation of specimens for DS tests has proven to be problematic and concerns have been raised at various of the participating laboratories regarding the ability of effectively ensure alignment of the various components and avoid the development of undesired bending effects.

ACKNOWLEDGEMENTS

The authors wish to acknowledge the financial assistance of the European Union for the Marie Curie Research Training Network En-Core, and the support of TG 9.3 of the International Federation for Structural Concrete (*fib*). Hughes Brothers and Fortius, Magmatech, Schock, ECC NV, S&P, Sika, and Sto Scandinavia AB are acknowledged for their participation in the RRT and for supplying the test materials.

REFERENCES

Chen, J.F., & Teng, J.G.. 2001. Anchorage strength models for FRP and steel plates bonded to concrete. *J. Struct. Eng.*, 127(7): 784–791.

Dai, J.G., Ueda, T. & Sato, Y. 2005. Development of the nonlinear bond stress-slip model of fiber reinforced plastics sheet-concrete interfaces with a simple method. *Journal of Composites for Construction*, 9(1): 52-62.

fib. 2001. *Bulletin 14 - Externally bonded FRP reinforcement for RC structures*. Lausanne: International Federation for Structural Concrete (*fib*)

Nakaba, K., Kanakubo, T., Furuta, T. & Yoshizawa, H. 2001. Bond Behavior between Fiber-Reinforced Polymer Laminates and Concrete. *ACI Structural Journal*, 98(3): 359-367.

Yao, J., Teng, J.G. & Chen, J.F. 2005. Experimental study on FRP-to-concrete bonded joints. *Composites: Part B*, 36(2): 99–113.

Williams, G., Al-Mahaidi, R. & Kalfat, R. 2010. The West Gate Bridge: Strengthening of a 20th Century Bridge for 21st Century Loading. *Fiber-Reinforced Polymer Reinforcement for Concrete Structures; Proc. of the 10th Intern. Symp.* ACI SP-275, Famington Hills, Michigan, USA.